

Deep inelastic events containing a forward photon as a probe of small x dynamics

J. Kwieciński¹, S. C. Lang and A. D. Martin,

Department of Physics, University of Durham, Durham, DH1 3LE, England

Abstract

We calculate the rate of producing deep inelastic events containing an energetic isolated forward photon at HERA. We quantify the enhancement arising from the leading $\log 1/x$ gluon emissions with a view to using such events to identify the underlying dynamics.

¹On leave from Henryk Niewodniczański Institute of Nuclear Physics, 31-342 Kraków, Poland.

1. Introduction

In the deep-inelastic small (Bjorken) x regime the gluon is the dominant partonic constituent of the proton, and the behaviour of the observables can be predicted in terms of the gluon distribution. At sufficiently small x it is necessary to resum the $\log 1/x$ contributions which, to leading-order accuracy, is accomplished by the BFKL equation [1] for the gluon distribution, $f(x, k_T^2)$, unintegrated over the gluon transverse momentum k_T . As x decreases the solution $f(x, k_T^2)$ is characterized by a singular $x^{-\lambda}$ growth accompanied by a diffusion in $\ln k_T^2$. To leading $\log 1/x$ accuracy, the “BFKL intercept” is $\lambda = (3\alpha_S/\pi) 4 \ln 2$ for fixed α_S (or $\lambda \approx 0.5$ if a reasonable prescription is used to allow α_S to run in the BFKL equation [2]). Sub-leading effects are expected to reduce the exponent.

The singular $x^{-\lambda}$ behaviour feeds through, via the k_T -factorization theorem, into the proton structure function $F_2(x, Q^2)$. Thus, in principle, measurements of F_2 at HERA should be able to determine λ . However, in practice it is difficult to distinguish the BFKL behaviour from that predicted by conventional DGLAP evolution, which resums $\alpha_S \log Q^2$ contributions. A major part of the problem is the necessity to provide non-perturbative input. Over the HERA regime, DGLAP evolution can mimic the steep $x^{-\lambda}$ growth by either taking a valence-like gluon $xg(x, Q_0^2) \rightarrow 0$ as $x \rightarrow 0$ at some sufficiently low input scale Q_0^2 [3], or by assuming an input form $xg(x, Q_0^2) \sim x^{-\lambda}$ as $x \rightarrow 0$ [4, 5]. Here $g(x, Q^2)$ is the conventional gluon distribution (integrated over k_T), namely

$$g(x, Q^2) = \int^{Q^2} \frac{dk_T^2}{k_T^2} f(x, k_T^2). \quad (1)$$

On the other hand, in the BFKL description of F_2 , there is a diffusion in $\ln k_T^2$ accompanying the translation of the input gluon $f(x, k_T^2)$ to smaller x values. This leads to a significant contribution from the infrared region which is beyond the scope of perturbative QCD and which has to be included phenomenologically.

Mueller [6] proposed an elegant way to overcome these ambiguities, and so sharpen up the theoretical description. He suggested that the study of deep-inelastic (x, Q^2) events which contain an identified energetic forward jet (x_j, k_{jT}^2) would, in principle, allow the identification of the $x^{-\lambda}$ behaviour, or to be precise the $(x/x_j)^{-\lambda}$ behaviour as $x/x_j \rightarrow 0$. The process is illustrated in Fig. 1(a)². Ideally we would select deep-inelastic events containing a jet whose transverse momentum k_{jT} is sufficiently large to suppress the diffusion into the infrared region, and with longitudinal momentum fraction x_j as large as experimentally feasible so that x/x_j

²Other properties of the final state have been proposed as possible ways to expose the mutual relationship between the steep power-like increase of the cross section and the lack of ordering in the transverse momenta of the gluon emissions along the chain. These include studies of (i) the transverse energy flow [7], (ii) the azimuthal decorrelation of two jets separated by a large rapidity gap [8, 9], and (iii) the azimuthal decorrelation of electro- or photo-produced dijets [10, 11]. The first tends to be masked by uncertainties due to hadronization and the other two by decorrelations which arise from other sources than $\log(1/x)$ resummation.

is as small as possible, typically $x_j > 0.05$. According to BFKL dynamics the differential structure function for this process has leading small x/x_j behaviour

$$\frac{\partial F_2}{\partial(\log 1/x_j) \partial k_{jT}^2} = C \alpha_S(k_{jT}^2) x_j \left[g + \frac{4}{9} (q + \bar{q}) \right] \left(\frac{x}{x_j} \right)^{-\lambda} \quad (2)$$

where the parton distributions (g, q and \bar{q}) are to be evaluated at (x_j, k_{jT}^2) — where they are well known. The normalisation coefficient C is given in refs. [12, 13, 14, 15]. Basically the idea is to try to identify the BFKL behaviour from deep-inelastic scattering off a known *parton* at large k_{jT}^2 , as opposed to scattering off a *proton* for which we need to specify its non-perturbative structure at small k_T^2 . In practice, however, the clean identification and kinematic measurement of a forward jet, closely adjacent to the proton remnants, poses a severe experimental challenge, particularly for jets at the smaller values of k_{jT}^2 where the DIS + jet events are more numerous. Nevertheless experimental studies [16] have been attempted with encouraging results, albeit for rather low values of k_{jT}^2 .

Here we study a related, but alternative process — namely deep-inelastic events containing an identified forward photon, see Fig. 1(b). As a probe of small x dynamics, the process DIS + γ has both advantages and disadvantages as compared to DIS + jet. A major advantage is that the measurement of a photon should be cleaner than that of a jet, and less ambiguous, particularly at the lower values of k_T . Moreover since the q or \bar{q} jet (denoted x'_q in Fig. 1(b)) is not identified we can enlarge the data sample by including events in which its constituents mingle with the proton remnants. On the other hand we expect the DIS + γ rate to be suppressed by a factor of order $\alpha/2\pi$ relative to DIS + jet, though we should gain a little back since the photon is easier to measure than the jet and the recoiling quark jet is not identified. A second disadvantage is that we require isolation of the photon so as to avoid events where it arises from the decay of a parent π^0 etc.

We first present (in Section 2) the QCD formalism necessary to calculate the cross section for the DIS + forward photon process at small x . Then in Section 3 we discuss the acceptance criteria to be applied to the outgoing photon. In Section 4 we quantify the DIS + γ event rate expected in the experiments at the HERA electron-proton collider. Finally Section 5 contains a brief discussion.

2. Basic QCD formula for the DIS + γ process

Here we study prompt photon production in deep-inelastic scattering at small x . That is the process

$$“\gamma” + p \rightarrow \gamma(x_\gamma, k_{\gamma T}) + X, \quad (3)$$

sketched in Fig. 1(b), in which the photon is identified in the final state. Deep inelastic events with small x and large x_γ offer an opportunity to identify the effects of the BFKL resummation

of the $\alpha_S \ln(x_\gamma/x)$ contributions, which arise from the sum over the real and virtual gluon emissions, such as the one depicted in Fig. 1(b). In analogy to the DIS + jet process, the advantage of process (3) is that the outgoing photon acts as a trigger to select events in which the deep-inelastic scattering occurs off a quark in a kinematic region where its distribution, $q(x_q, k_{\gamma T}^2)$, is known.

The differential structure functions for this process may be written in the form

$$\frac{\partial^2 F_i}{\partial x_\gamma \partial k_{\gamma T}^2} = \int \frac{d^2 k_{gT}}{\pi k_{gT}^4} \int \frac{dx_q}{x_q} \Phi_i \left(\frac{x}{x_q}, k_{gT}^2, Q^2 \right) \sum_q e_q^2 \left[q(x_q, k_{\gamma T}^2) + \bar{q}(x_q, k_{\gamma T}^2) \right] \frac{|\mathcal{M}|^2}{z_\gamma z'_q} \quad (4)$$

for $i = T, L$. The variables are indicated on Fig. 1(b) and are defined below. The region of integration in (4) will be specified later. The subprocess $q(k_q) + g(k_g) \rightarrow q(k'_q) + \gamma(k_\gamma)$ (and also $\bar{q}g \rightarrow \bar{q}\gamma$) is described by the two Feynman diagrams shown in Fig. 2. It has matrix element squared

$$|\mathcal{M}|^2 = 2 C_2(F) \frac{\alpha_S(k_{\gamma T}^2)}{2\pi} \frac{\alpha}{2\pi} \frac{k_{gT}^2 [1 + (1 - z_\gamma)^2]}{\hat{s}(-\hat{u})} \quad (5)$$

where $C_2(F) = 4/3$ and the invariants \hat{s} and \hat{u} are

$$\hat{s} = (k_\gamma + k'_q)^2, \quad \hat{u} = (k_q - k_\gamma)^2. \quad (6)$$

The fractional momenta x_i in (4) are defined by the Sudakov decomposition of the particle 4-momenta

$$k_i = x_i p' + \beta_i q' + \mathbf{k}_{iT} \quad (7)$$

where at high energies p' and q' are to a good approximation the light-like 4-momenta associated with the incoming proton and virtual photon respectively

$$p' \equiv p - \frac{M^2}{2p \cdot q} q, \quad q' \equiv q + xp, \quad (8)$$

where M is the mass of the proton. The variables z_i in (4) and (5) are given by

$$z_i = x_i / x_q. \quad (9)$$

The 4-momenta of the outgoing photon and quark jet satisfy the on-mass-shell condition $k_i^2 = 0$ which gives

$$\beta_i = \frac{x}{x_i} \frac{k_{iT}^2}{Q^2} \quad (10)$$

for $i = \gamma$ or the outgoing quark q' .

The functions $\Phi_i(z, k^2, Q^2)$ in (4) describe the gluon chain which couples to the incoming virtual photon. The function Φ_T corresponds to the function F in ref. [14]. To be precise, the factors Φ_i/k^2 can be identified with the virtual gluon structure functions integrated over the

longitudinal momentum of the gluon. They can be obtained from the BFKL equation with the boundary condition given by the quark box (and “crossed” box) contributions. That is

$$\begin{aligned}\Phi_i(z, k^2, Q^2) &= \Phi_i^{(0)}(z, k^2, Q^2) + \\ &+ \frac{3\alpha_S}{\pi} k^2 \int_z^1 \frac{dz'}{z'} \int_0^\infty \frac{dk'^2}{k'^2} \left[\frac{\Phi_i(z', k'^2, Q^2) - \Phi_i(z', k^2, Q^2)}{|k'^2 - k^2|} + \frac{\Phi_i(z', k^2, Q^2)}{\sqrt{4k'^4 + k^4}} \right]\end{aligned}\quad (11)$$

where the inhomogeneous or driving terms $\Phi_i^{(0)}$ correspond to the sum of the quark box and crossed-box contributions. At small z we have

$$\Phi_i^{(0)}(z, k^2, Q^2) \approx \Phi_i^{(0)}(z=0, k^2, Q^2) \equiv \Phi_i^{(0)}(k^2, Q^2) \quad (12)$$

where

$$\begin{aligned}\Phi_T^{(0)}(k^2, Q^2) &= 2 \sum_q e_q^2 \frac{Q^2}{4\pi^2} \alpha_S \int_0^1 d\beta \int d^2\kappa [\beta^2 + (1-\beta)^2] \left(\frac{\kappa^2}{D_1^2} - \frac{\boldsymbol{\kappa} \cdot (\boldsymbol{\kappa} - \mathbf{k})}{D_1 D_2} \right) \\ \Phi_L^{(0)}(k^2, Q^2) &= 2 \sum_q e_q^2 \frac{Q^4}{\pi^2} \alpha_S \int_0^1 d\beta \int d^2\kappa \beta^2 (1-\beta)^2 \left(\frac{1}{D_1^2} - \frac{1}{D_1 D_2} \right)\end{aligned}\quad (13)$$

with the denominators D_i given by

$$\begin{aligned}D_1 &= \kappa^2 + \beta(1-\beta) Q^2 \\ D_2 &= (\boldsymbol{\kappa} - \mathbf{k})^2 + \beta(1-\beta) Q^2.\end{aligned}\quad (14)$$

The BFKL equation, (11), has been written for fixed QCD coupling α_S . In this case the leading small x behaviour of the solution can be given analytically. We have

$$\begin{aligned}\Phi_T(z, k^2, Q^2) &= \frac{9\pi^2}{512} \frac{2 \sum e_q^2 \alpha_S^{\frac{1}{2}}}{\sqrt{21\zeta(3)/2}} (k^2 Q^2)^{\frac{1}{2}} \frac{z^{-\alpha_P+1}}{\sqrt{\ln(1/z)}} \left[1 + \mathcal{O} \left(\frac{1}{\ln(1/z)} \right) \right] \\ \Phi_L(z, k^2, Q^2) &= \frac{2}{9} \Phi_T(z, k^2, Q^2)\end{aligned}\quad (15)$$

where we have omitted the Gaussian diffusion factor in $\ln(k^2/Q^2)$. The Riemann zeta function $\zeta(3) = 1.202$, and α_P , the celebrated BFKL intercept, is given by

$$\alpha_P - 1 = \frac{12\alpha_S}{\pi} \ln 2. \quad (16)$$

In practice we allow the coupling α_S to run, following the prescription of ref. [14]. That is we solve the BFKL equations for

$$H_i(z, k^2, Q^2) = \frac{3\alpha_S(k^2)}{\pi} \Phi_i(z, k^2, Q^2). \quad (17)$$

Actually we solve the differential form of the equations

$$\frac{\partial H_i(z, k^2, Q^2)}{\partial \log(1/z)} = \frac{3\alpha_S(k^2)}{\pi} k^2 \int_{k_0^2}^{\infty} \frac{dk'^2}{k'^2} \left[\frac{H_i(z, k'^2, Q^2) - H_i(z, k^2, Q^2)}{|k'^2 - k^2|} + \frac{H_i(z, k^2, Q^2)}{\sqrt{4k'^4 + k^4}} \right] \quad (18)$$

subject to the boundary conditions

$$H_i(z = z_0, k^2, Q^2) = H_i^{(0)}(k^2, Q^2) \quad (19)$$

where we choose $z_0 = 0.1$ and the cut-off $k_0^2 = 1 \text{ GeV}^2$. For any small z the solutions $H_i(z, k^2, Q^2)$ therefore only depend on the behaviour of H_i in the interval (z, z_0) . We impose the same cut, $x/x_q < 0.1$, in the x_q integration in (4). Of course the integration is also subject to the kinematic constraint $x_q > x_\gamma$. We find that the slope $\lambda = \alpha_P - 1$ and the overall normalization of the solution of the BFKL equation with running coupling α_S are in general smaller than those obtained with fixed coupling $\alpha_S(Q^2)$.

We are now in a position to calculate the differential structure function $\partial F_2 / \partial x_\gamma \partial k_{\gamma T}^2$ from (4). We compute it first using Φ_2 obtained from solving the BFKL equation (18) and then repeat the calculation using for Φ_2 just the driving (quark box) term $\Phi_2^{(0)}$. The difference between the two calculations is a measure of the effect of the BFKL resummation of soft gluon emissions. The result for the F_2 differential structure function is shown in Fig. 3 as a function of x_γ for three different values³ of x . We see that the difference between the BFKL and quark box results is dramatic once x is sufficiently small ($x \lesssim 10^{-3}$) and provided $x_\gamma \sim 0.1$. Indeed we require x/x_γ to be small for the formalism to be valid. As explained in ref. [14] it is the shape rather than the magnitude of $\partial F_i / \partial x_\gamma \partial k_{\gamma T}^2$ which is the more reliable discriminator of the underlying dynamics at small x , since the normalization of the QCD predictions is subject to uncertainties arising mainly from the regions of low transverse momenta.

Fig. 3 for the differential structure function for DIS + γ events should be compared with a similar figure for DIS + jet events shown in Fig. 7 of ref. [14]. We see that the cross section is about a factor of 1000 lower for the photon process, as could be anticipated from the presence of the extra $\alpha/2\pi$ coupling of the photon. In the next section we will impose reasonable experimental cuts on the outgoing photon, and then we will quantify the event rate which may be observed at HERA.

3. Cuts to select the DIS + photon events

We are interested in semi-inclusive deep inelastic events in which only the photon is measured in the final state, besides the scattered electron. On the other hand the integrals defining the

³The result using $\Phi_2 = \Phi_2^{(0)}$ is independent of x (until we reach the kinematic limit $\beta_\gamma = 1$), and its shape in x_γ reflects the quark and antiquark distributions in the proton after integration over x_q . In contrast for DIS + jet the x_j shape of the box contribution is dominated by the gluon distribution $x_j g(x_j, k_{jT}^2)$, that is the gluon is sampled “locally”.

differential structure functions, (4), contain a potential singularity at $\hat{s} = 0$ which has to be regularized by a suitably chosen cut-off. A straightforward limitation of the region of integration to $\hat{s} > s_0$, where s_0 is some arbitrarily chosen value, is therefore not possible for making a direct comparison of (4) with experiment, since \hat{s} is only determined if the recoil quark jet q' were to be detected as well as the photon. However, it is necessary to impose an isolation cut on the outgoing photon to distinguish it from background photons which arise from the decay of π^0 's produced either from the proton remnants or the outgoing quark jet, q' . Suppose we impose an isolation angle θ_0 (where θ_0 is chosen to be around, say, 3° – 10°) defining a cone around the photon, then at the parton level we have $\theta_{\gamma q'} > \theta_0$ and hence a corresponding lower limit on \hat{s} , since

$$\hat{s} > 2E_\gamma E_{q'} (1 - \cos \theta_{\gamma q'}). \quad (20)$$

A second requirement is that our photon should be emitted in the proton hemisphere in the virtual photon-proton c.m. frame to avoid contamination from photons radiated from the quark-antiquark pair which form the quark box. Thus we require

$$x_\gamma > \beta_\gamma \quad (21)$$

which on using (10), gives

$$x_\gamma > \sqrt{x k_{\gamma T}^2 / Q^2}. \quad (22)$$

The hemisphere cut, when combined with the kinematic constraint $x_q > x_\gamma$, imposes an implicit lower limit of the x_q integration in (4)

$$x_q > x_\gamma > \sqrt{x k_{\gamma T}^2 / Q^2}. \quad (23)$$

We see that this limit is generally stronger than our BFKL requirement that $x_q > 10x$.

Finally there is the practical limitation that photons can only be measured if they are emitted at sufficiently large angles to the proton beam direction in the HERA laboratory frame, say

$$\theta_{\gamma p} > \bar{\theta}_0. \quad (24)$$

The allowed regions of the kinematic variables $(x_\gamma, k_{\gamma T}^2)$ describing the photon are shown in Fig. 3 for various choices of $\bar{\theta}_0$. We see that large x_γ photons are only emitted at small $\theta_{\gamma p}$; for a given $\theta_{\gamma p}$ we can reach larger x_γ by observing photons with large $k_{\gamma T}^2$, but then the event rate is depleted. We also show on Fig. 3 the “forward hemisphere” boundary, (22), for $x = 6 \times 10^{-4}$ and $Q^2 = 20 \text{ GeV}^2$.

4. Predictions for DIS + photon production

Here we present the numerical predictions for the cross section for the production of an energetic photon in the deep inelastic ep scattering taking into account various cuts discussed in the previous section. The relevant cross section is given by the following formula:

$$\frac{d\sigma}{dx_\gamma dk_{\gamma T}^2 dx dQ^2} = \frac{4\pi\alpha^2}{Q^4 x} \left[(1-y) \frac{dF_2}{dx_\gamma dk_{\gamma T}^2} + \frac{y^2}{2} \frac{dF_T}{dx_\gamma dk_{\gamma T}^2} \right]. \quad (25)$$

We show in Fig. 5 the dependence of the integrated cross section on the variation of (a) the angle θ_0 defining the photon isolation cone and (b) the $k_{\gamma T}^2$ threshold for photon detection. We see that the dependence on the isolation cone angle is relatively weak.

In Fig. 6 we show the integrated cross section for prompt forward photon production as a function of x for three different Q^2 bins: 20-30, 30-40 and 40-50 GeV^2 respectively. We compare the predictions for the case where the BFKL small x resummation is incorporated with those where the gluon radiation is neglected. The x dependence of the cross section is driven by the small z behaviour of the Φ_i . The results show a strong enhanced increase with decreasing x which is characteristic of the effect of soft gluon resummation. At $x \approx 10^{-4}$ the cross section is about a factor of 3.5 larger than that in which the BFKL effects are neglected. Since the impact factors, $\Phi_i^{(0)}$, are independent of x , the weak x dependence in the latter case arises mainly from acceptance. Finally in Fig. 7 we show the cross section in the various deep inelastic (x, Q^2) bins. The values are shown in fb and so would correspond to the number of events for an eventual integrated luminosity of 1 fb^{-1} .

The DIS + γ cross sections presented in Figs. 6 and 7 may be compared directly with the values for the DIS + jet process shown in Fig. 4 of [15] and Fig. 8 of [17] respectively. We see that there is a suppression of about a factor of 400 in going from the DIS + jet to the DIS + γ process. Of course the ratio depends on the precise cuts that are imposed in each case. In table 1 we show the effect on the DIS + γ cross section in one of the $\Delta x, \Delta Q^2$ bins of varying $\bar{\theta}_0$ (the minimum angle to the proton beam) and θ_0 (the half-angle of the isolation cone). We see that the event rate is less sensitive to the cone angle θ_0 than to the minimum angle $\bar{\theta}_0$ to the beam.

Table 1: The DIS + γ cross section in the bin $6 \times 10^{-4} < x < 8 \times 10^{-4}$, $20 < Q^2 < 30 \text{ GeV}^2$ as calculated in Fig. 7, but for different choices of $\bar{\theta}_0$ and θ_0 .

$\bar{\theta}_0$	θ_0	$\Delta\sigma \text{ (fb)}$
5°	3°	46.2
7°	3°	29.1
7°	5°	26.2

5. Discussion

The DIS + jet process is, in principle, an ideal way to probe small x dynamics, *provided* sufficiently forward jets can be measured. In practice to separate cleanly such forward jets from the proton remnants is a formidable challenge. Here we have studied the analogous DIS + γ process which has the advantage that forward photons can be more reliably measured than forward jets, but for which the event rate is considerably suppressed. In section 4 we quantified the suppression. There we predicted the DIS + γ cross section using BFKL dynamics and found a characteristic rise with decreasing x , which becomes steeper the more forward are the detected photons.

Our study should be regarded as an exploratory investigation of the potential usefulness of the process. The DIS + γ rates which we present in Figs. 6 and 7 correspond to photons produced (i) at more than 5° to the proton beam direction ($\theta_{\gamma p} > \bar{\theta}_0 = 5^\circ$) in the HERA frame, (ii) in the centre of an isolation cone of half-angle 3° ($\theta_{\gamma q'} > \theta_0 = 3^\circ$) in the HERA frame, (iii) in the proton hemisphere in the γ^*p c.m. frame (to avoid contamination with photons radiated from the quark box), and (iv) with $k_{\gamma T}^2 > 5 \text{ GeV}^2$. Our work is at the parton level and so in practice the isolation criteria will need further study. In particular simulations of the fragmentation of the outgoing (q') jet should be performed so as to be able to choose the optimum isolation criteria for the photon. Recall that isolation is required to suppress (background) photons from π^0 decays.

There is a second reason why it is important to know the rate of DIS + forward photon events. We have stressed the experimental difficulty of obtaining a clean sample of DIS events containing a measured forward jet close to the proton remnants. An alternative possibility to expose $\log(1/x)$ resummation effects is to use the improved knowledge of the fragmentation functions to identify the forward jet through the measurement of a single energetic decay product. As it happens the π^0 is the hadron which can be identified in the most forward direction in the detectors at HERA. For this alternative signal of small x dynamics, our process is then the background.

Acknowledgements

We thank Albert De Roeck, Genya Levin and Peter Sutton for valuable help and discussions. J.K. thanks the Department of Physics and Grey College of the University of Durham for their warm hospitality. This work has been supported in part by Polish KBN Grant No. 2 P03B 231 08 and the EU under Contracts Nos. CHRX-CT92-0004 and CHRX-CT93-0357. SCL thanks the UK Engineering and Physical Sciences Research Council for a Studentship.

References

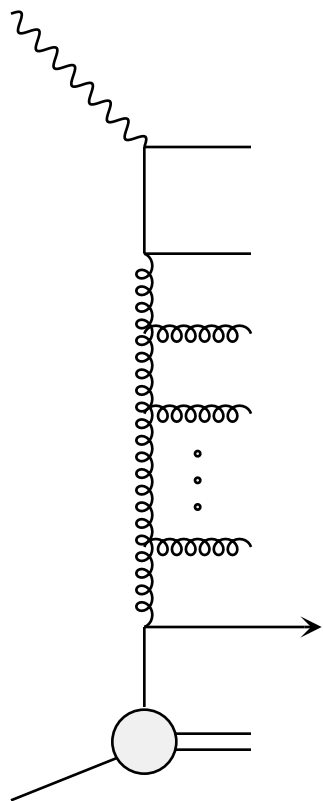
- [1] E. A. Kuraev, L. N. Lipatov and V. Fadin, Zh. Eksp. Teor. Fiz. **72**, 373 (1977) (Sov. Phys. JETP **45**, 199 (1977));
Ya. Ya. Balitzkij and L. N. Lipatov, Yad. Fiz. **28**, 1597 (1978) (Sov. J. Nucl. Phys. **28**, 822 (1978));
L. N. Lipatov, in “Perturbative QCD”, edited by A. H. Mueller, (World Scientific, Singapore, 1989), p. 441;
J. B. Bronzan and R. L. Sugar, Phys. Rev. **D17**, 585 (1978);
T. Jaroszewicz, Acta. Phys. Polon. **B11**, 965 (1980).
- [2] A. J. Askew, J. Kwiecinski, A. D. Martin and P. J. Sutton, Phys. Rev. **49** (1994) 4402.
- [3] M. Glück, E. Reya and A. Vogt, Z. Phys. **C67** (1995) 433.
- [4] A. D. Martin, R. G. Roberts and W. J. Stirling, Phys. Rev. **D50** (1994) 6734; Phys. Lett. **B354** (1995) 155.
- [5] CTEQ collaboration: H. Lai et al., Phys. Rev. **D51** (1995) 4763.
- [6] A. H. Mueller, Nucl. Phys. B (Proc. Suppl.) **18C** (1990) 125; J. Phys. **G17** (1991) 1443.
- [7] K. Golec-Biernat, J. Kwiecinski, A. D. Martin and P. J. Sutton, Phys. Rev. **D50** (1994) 217; Phys. Lett. **B335** (1994) 220.
- [8] V. Del Duca and C. R. Schmidt, Phys. Rev. **D51** (1995) 2150.
- [9] W. J. Stirling, Nucl. Phys. **B423** (1994) 56.
- [10] J. R. Forshaw and R. G. Roberts, Phys. Lett. **B335** (1994) 494.
- [11] A. J. Askew, D. Graudenz, J. Kwiecinski and A. D. Martin, Phys. Lett. **B338** (1994) 92.
- [12] W. K. Tang, Phys. Lett. **B278** (1992) 363.
- [13] J. Bartels, A. De Roeck and M. Loewe, Z. Phys. **C54** (1992) 635; Nucl. Phys. B (Proc. Suppl.) **29A** (1992) 61.
- [14] J. Kwiecinski, A. D. Martin and P. J. Sutton, Phys. Rev. **D46** (1992) 921.
- [15] J. Kwiecinski, A. D. Martin and P. J. Sutton, Phys. Lett. **B287** (1992) 254.
- [16] H1 collaboration: S. Aid et al., Phys. Lett., **B356** (1995) 118;
J. Bartels et al., DESY preprint 96-036.
- [17] J. Kwiecinski, A. D. Martin and P. J. Sutton, Nucl. Phys. B (Proc. Suppl.) **29A** (1992) 67.

Figure Captions

- Fig. 1 Diagrammatic representation of (a) a deep-inelastic + forward jet event, and (b) a deep-inelastic (x, Q^2) + forward identified photon $(x_\gamma, k_{\gamma T})$ event.
- Fig. 2 The Feynman diagrams describing the $gq \rightarrow \gamma q$ subprocess embodied in the DIS + γ diagram shown in Fig. 1(b).
- Fig. 3 The F_2 differential structure function, (4), for deep-inelastic (x, Q^2) events accompanied by a measured forward photon $(x_\gamma, k_{\gamma T}^2)$ as a function of x_γ for different values of x , $x = 10^{-4}$, 10^{-3} and 10^{-2} , and for $Q^2 = 5 \text{ GeV}^2$. The continuous curves correspond to inputting into (4) the solution Φ_2 of the BFKL equation (18), whereas the dashed curve is calculated using for Φ_2 simply the driving term $\Phi_2^{(0)}$ of (19). Here $|\mathcal{M}|^2$ is regulated by requiring $\hat{s} > 1 \text{ GeV}^2$. Plots (a) and (b) correspond to photons with $k_{\gamma T}^2 = 5$ and 10 GeV^2 respectively.
- Fig. 4 The curves give the *upper* boundary of the allowed regions of the photon kinematic variables $(x_\gamma, k_{\gamma T}^2)$ for deep-inelastic + photon events with $x = 6 \times 10^{-4}$ and $Q^2 = 20 \text{ GeV}^2$ for various choices of the acceptance angle $\bar{\theta}_0$ of (24). The photon angle $\bar{\theta}_0$ to the proton direction in the HERA ($30 \times 820 \text{ GeV}$) laboratory frame is not uniquely specified by $(x, Q^2; x_\gamma, k_{\gamma T}^2)$. Varying the remaining azimuthal angle transforms the line of constant $\theta_{\gamma p}$ into narrow bands in the $x_\gamma, k_{\gamma T}^2$ plane. The continuous lines that are shown are obtained by averaging over the azimuthal degree of freedom. The lines are insensitive to reasonable variations of x and Q^2 . Also shown (by a dashed line) is the *lower* boundary given by the hemisphere cut (22) for $x = 6 \times 10^{-4}$ and $Q^2 = 20 \text{ GeV}^2$.
- Fig. 5 The dependence of the DIS + γ cross section integrated over the photon variables to variation of (a) the angle θ_0 defining the isolation cone around the photon ($\theta_{\gamma j} > \theta_0$) and (b) the threshold for photon detection ($k_{\gamma T}^2 > k_{th}^2$). The results are for the x, Q^2 bin defined by $6 \times 10^{-4} < x < 8 \times 10^{-4}$ and $20 < Q^2 < 30 \text{ GeV}^2$. We impose the hemisphere cut (23) and take $\bar{\theta}_0 = 5^\circ$ in (24). (The lack of smoothness of the curves simply reflects the errors on the six-fold numerical integration).
- Fig. 6 The cross section, $\langle \sigma \rangle$ in pb, for deep inelastic + photon events integrated over $\Delta x = 2 \times 10^{-4}$, $\Delta Q^2 = 10 \text{ GeV}^2$ bins which are accessible at HERA, and integrated over the region $\theta_{\gamma p} > 5^\circ$, $k_{\gamma T}^2 > 5 \text{ GeV}^2$, but subject to (23) and an isolation cut of $\theta_0 = 3^\circ$. The x dependence is shown for three different ΔQ^2 bins, namely (20,30), (30,40) and (40,50) GeV^2 . The $\langle \sigma \rangle$ values are plotted at the central x value in each Δx bin and joined by straight lines. The continuous curves show $\langle \sigma \rangle$ calculated with Φ_i determined from the BFKL equation, whereas the dashed curves are obtained just from the driving terms $\Phi_i^{(0)}$, i.e. from the quark box. For clarity a vertical line links the pair of curves belonging to the same ΔQ^2 bin.

Fig. 7 The cross section $\langle\sigma\rangle$ in fb for deep inelastic + photon events in various $(\Delta x, \Delta Q^2)$ bins which are accessible at HERA, and integrated over the region $\theta_{\gamma p} > 5^\circ$, $k_{\gamma T}^2 > 5 \text{ GeV}^2$, but subject to (23) and an isolation cut of $\theta_0 = 3^\circ$. The number in brackets is the cross section calculated with just the quark box approximation ($\Phi_i = \Phi_i^{(0)}$). The difference between the two numbers is therefore the enhancement due to the BFKL soft gluon resummation.

(a) DIS + jet



(b) DIS + γ

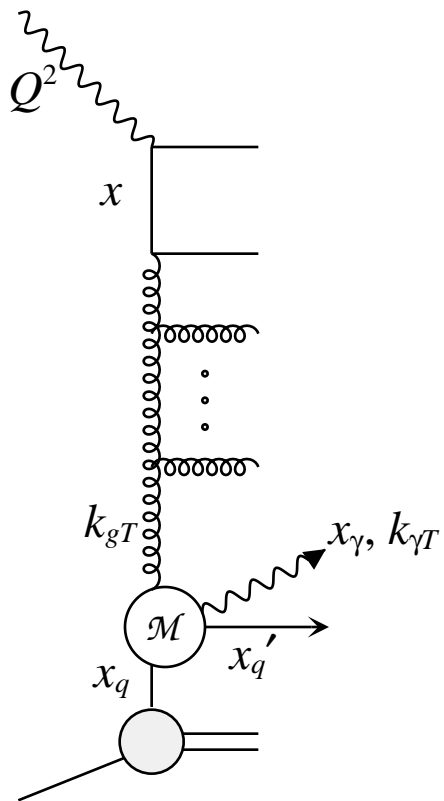


Fig.1

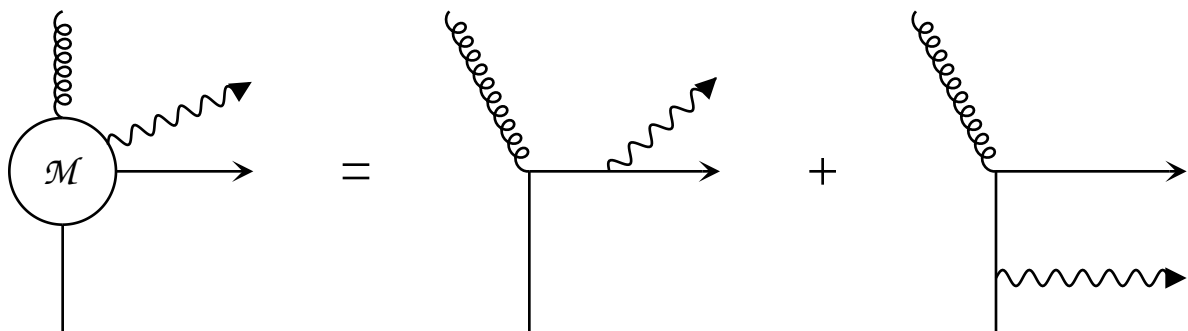


Fig.2

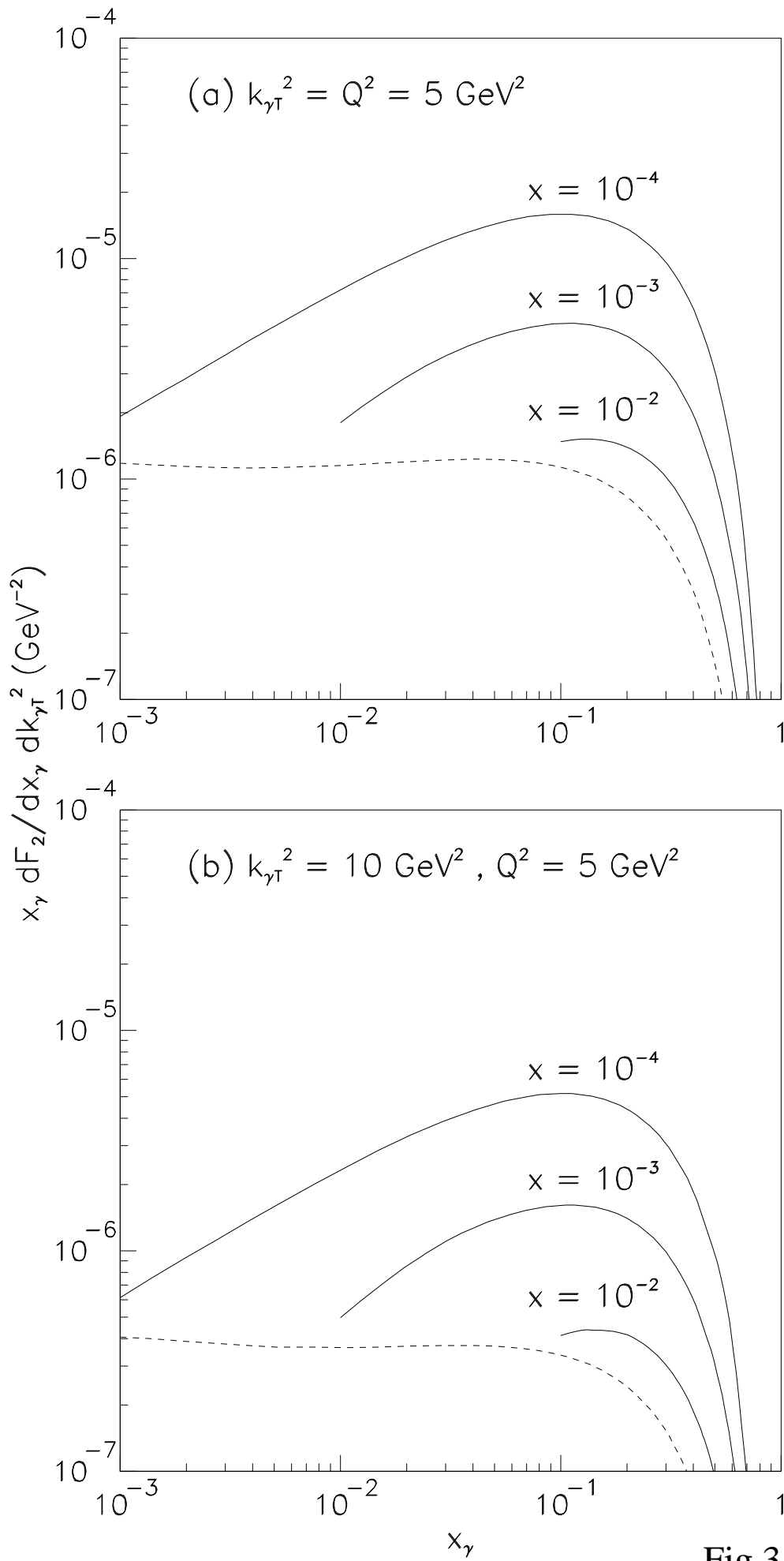


Fig.3

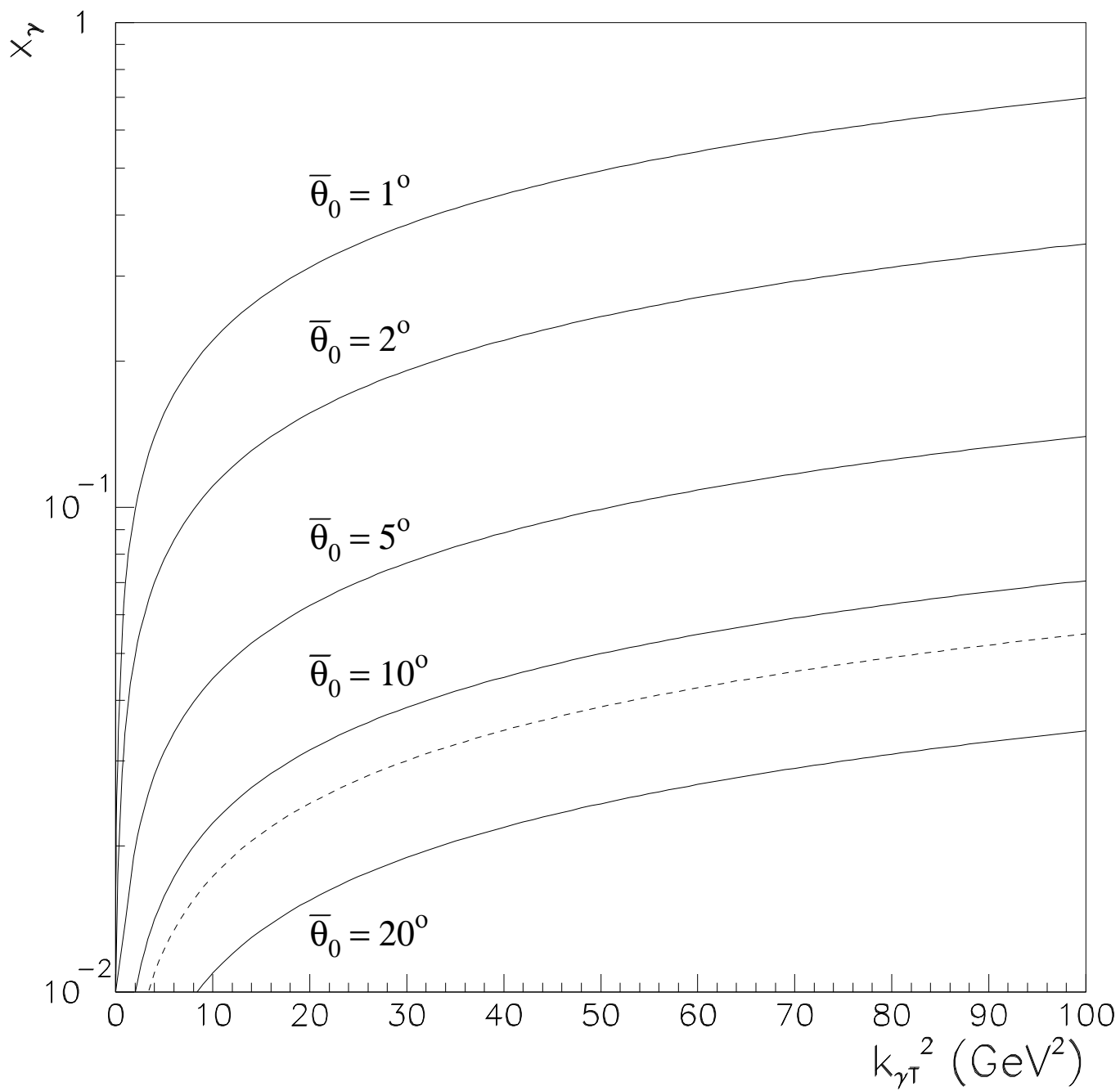


Fig.4

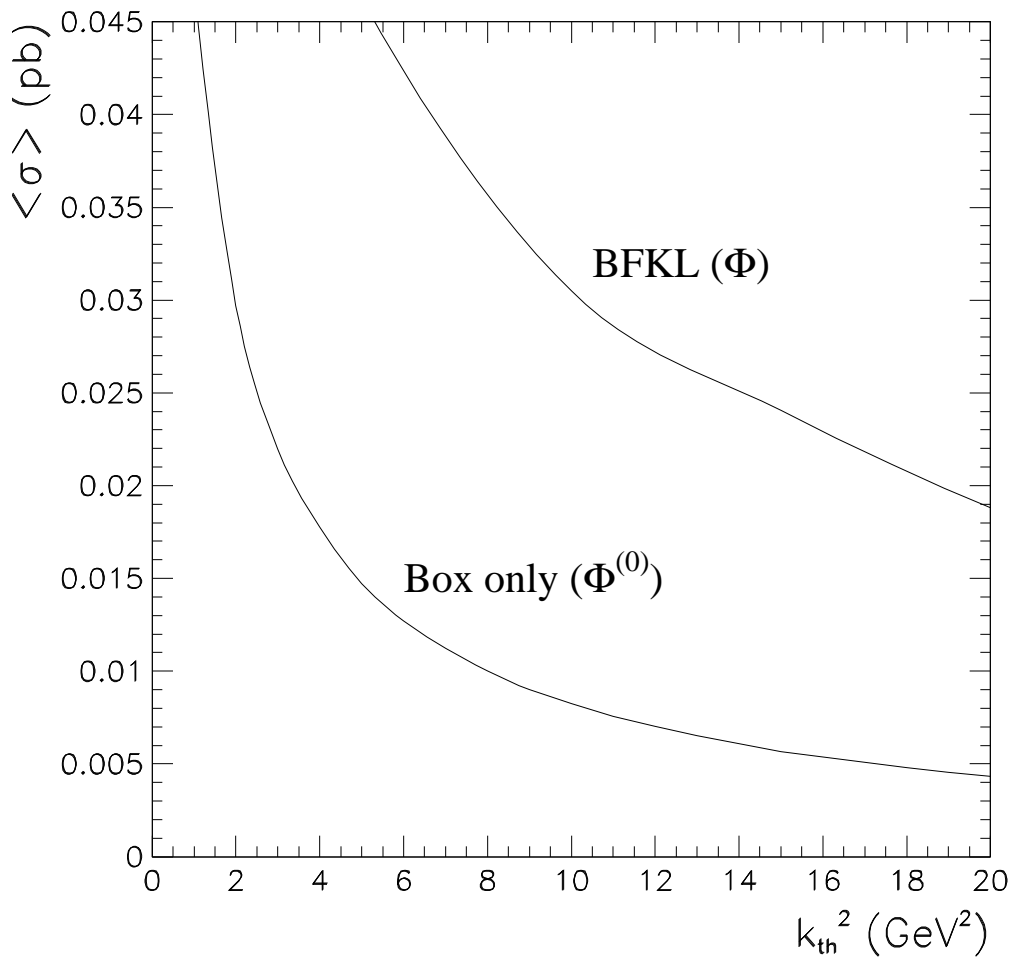
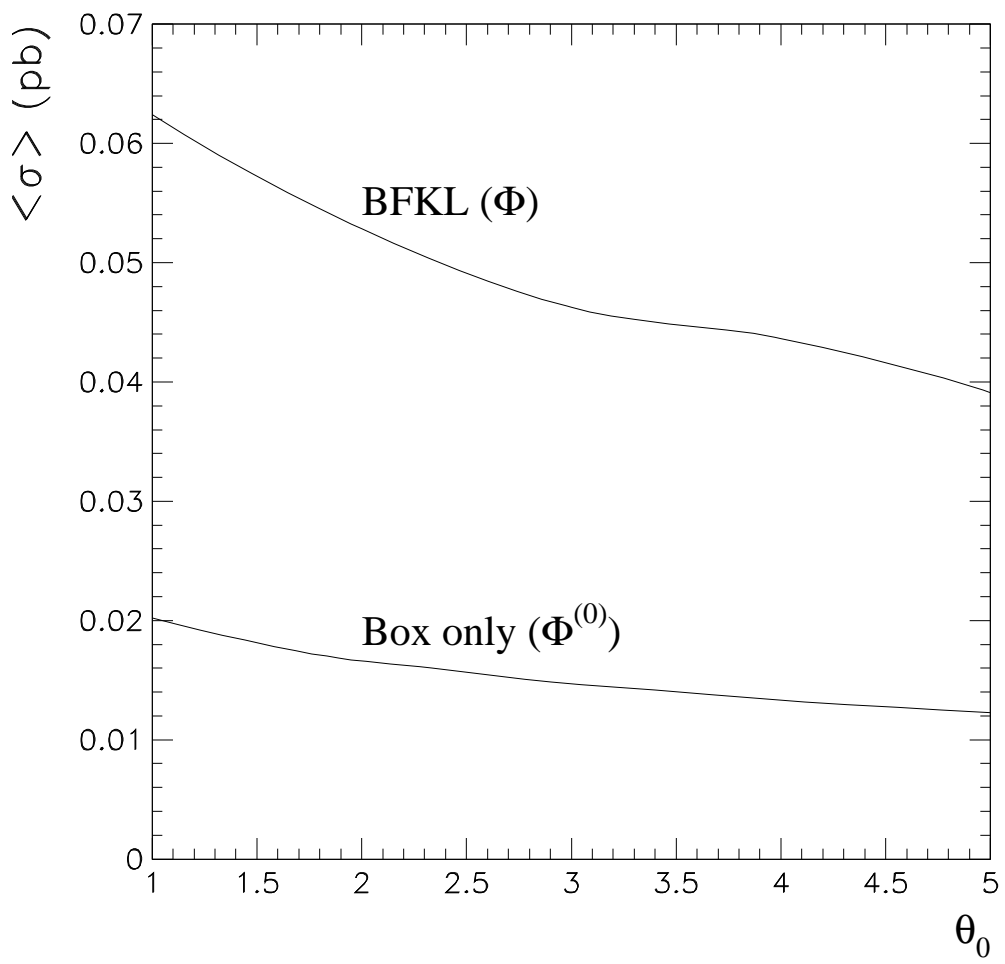


Fig.5

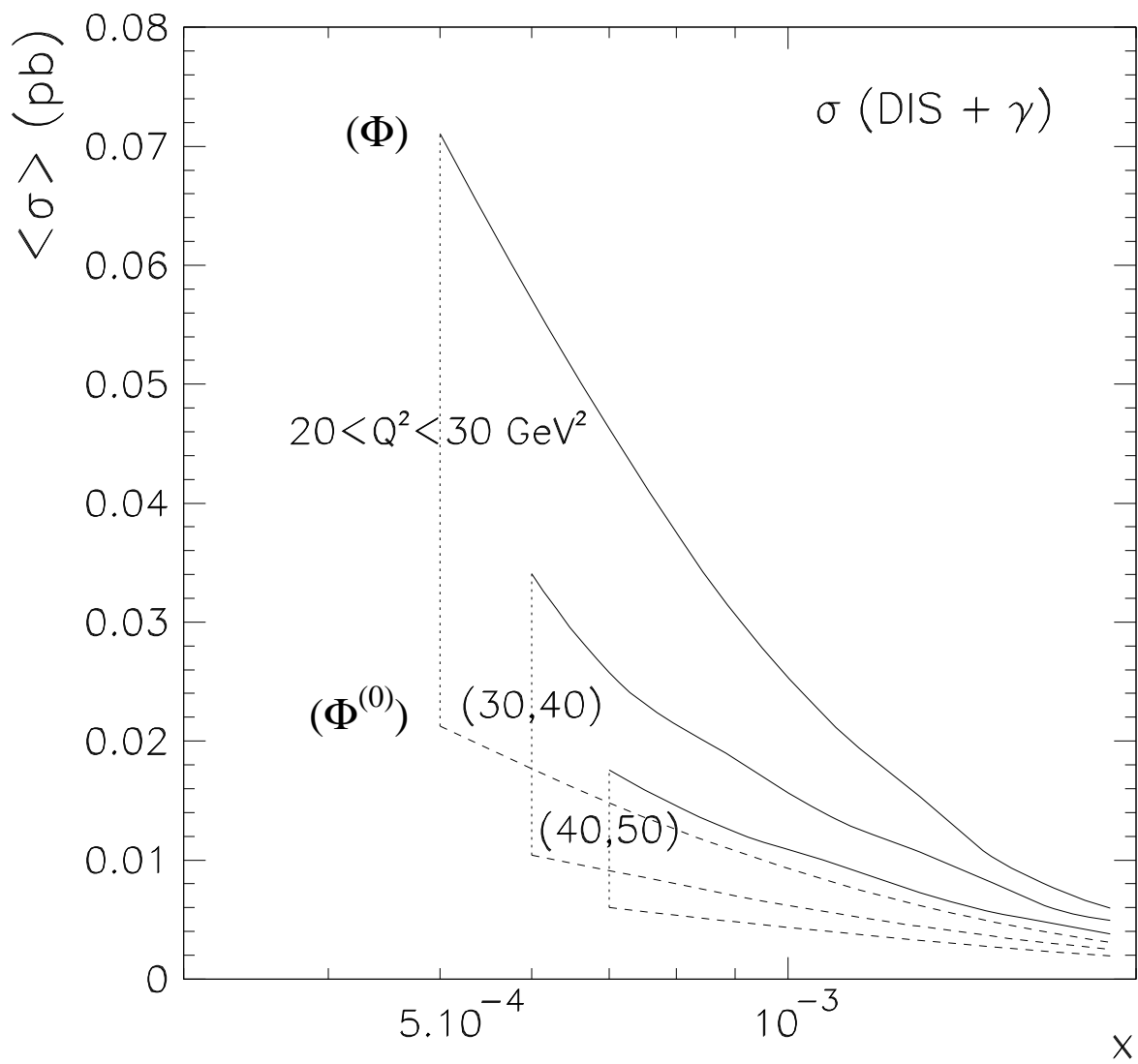


Fig.6

